

A Channel Estimation Framework for High-mobility FDD Massive MIMO using Partial Reciprocity

Ziao Qin*, Haifan Yin*, David Gesbert[†]

*School of Electronic Information and Communications,

Huazhong University of Science and Technology, 430074 Wuhan, China

[†]Communications Systems Department, EURECOM, 06904 Biot, France

Email: ziao_qin@hust.edu.cn, yin@hust.edu.cn, gesbert@eurecom.fr

Abstract—The estimation of Channel State Information (CSI) is one of the most difficult tasks for massive multiple-input multiple-output (MIMO) in frequency division duplex (FDD) mode. It is even more challenging in high-mobility scenarios. In this paper, we consider an FDD massive MIMO system with high-mobility and CSI delay and aim to predict the downlink (DL) channel under a realistic multipath channel model. The key novelty lies in the fact that for the first time we devise a joint angle-delay-Doppler (JADD) channel estimation framework. The main idea of our framework is to reconstruct the DL channel with the DL channel parameters estimated from the uplink (UL) channel samples and scalar feedback coefficients. To alleviate the feedback overhead, we design a wideband beamformer for the base station (BS) based on the DL angle-delay-Doppler parameters. The user equipment (UE) then estimates the DL channel parameters and feeds back some Doppler-related scalar coefficients back to the BS. We show that the feedback and DL pilot training overhead are independent of the number of BS antennas. The lower bound performance of our framework is also derived. Numerical results under the industrial channel model in rich scattering environments demonstrate that our framework works well from medium mobility scenario of 30 km/h to high mobility settings of 350 km/h.

Index Terms—Massive MIMO, curse of mobility, FDD, beamforming, Matrix Pencil, 5G.

I. INTRODUCTION

Massive MIMO is one of the key technologies in the fifth generation (5G) cellular communication systems [1]. In order to fully exploit the merits of massive MIMO, such as spectral efficiency (SE) and energy efficiency (EE) [2], CSI acquisition is vital. In TDD mode, the channel reciprocity facilitates the estimation of DL CSI [3]. Unfortunately, the different operating frequency band in FDD leads to non-reciprocal channels. Therefore, the overhead of feedback and channel training usually scale with the number of BS antennas. The reduction of this overhead in massive MIMO was addressed in literature, e.g., by [4] with compressed sensing (CS). Another performance bottleneck in massive MIMO is mobility [5]. The Doppler effect in mobile scenarios is inevitable and becomes nontrivial as the mobility increases. Timely CSI acquisition is extremely important in high-mobility scenarios. Some works focused on solving the mobility problem in TDD mode using Prony's method [6], maximum likelihood method [7] and

deep learning method [8]. The authors in [9] also offers a parameter-tracking way to reconstruct the DL channel. In real FDD massive MIMO system with high mobility, CSI acquisition is much more difficult than in stationary setting because of the fast-varying channel and CSI delay. Few works focus on solving the CSI acquisition problem in FDD massive MIMO with high-mobility under a practical multi-path channel model such as the one used in current standardization [10]. Traditional methods, e.g., those based deep learning and CS may not directly apply in this case because of the time-varying nature of the channel demands for timely CSI updating and low-complexity channel prediction algorithm.

In this paper, we address the CSI acquisition problem in high-mobility FDD massive MIMO with a novel partial reciprocity-based CSI reconstruction framework, which targets at solving the mobility problem and reducing the feedback overhead. Although the full-reciprocity in FDD does not hold, the frequency-unrelated channel parameters of UL and DL are reciprocal [11]–[13]. More specifically, we propose a polynomial-complexity channel reconstruction framework based on partial channel reciprocity. A linear method called Matrix Pencil [14] is introduced to estimate the Doppler frequency of the UL channel. Thanks to the channel sparsity in spatial-frequency domain, the complexity of UL parameter estimation can be reduced. The partial channel reciprocity enables us to estimate the UL channel parameters and computes the DL parameters using UL ones. With the acquired DL channel parameters, we propose a wideband beamformer which depends on spatial-frequency-Doppler channel parameters. This beamformer not only helps reducing the DL pilot training overhead but also facilitate UEs to feed back scalar coefficients to the BS. Our beamformer differs from the traditional ones as it depends on the estimation of angle-delay-Doppler channel parameters simultaneously at the BS and the UE. The mobility problem is also dealt with conveniently, since the DL channel is reconstructed at the BS with slow-varying parameters estimated by our framework. Our framework is capable of predicting the channel in polynomial complexity and it outperforms traditional methods which typically are based on the NP-hard solutions or failing to timely update CSI.

Under the 3rd Generation Partner Project (3GPP) multipath channel model, numerical results show that JADD in high mo-

This work was supported by National Natural Science Foundation of China under Grant 62071191.

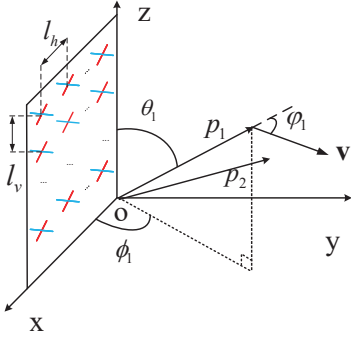


Fig. 1. UPA antenna configuration in 3D-Cartesian coordinate system.

bility scenarios outperforms existing methods in standardization [15]. The robustness of our framework to large CSI delays, e.g., up to 10 ms, is also demonstrated in our simulation.

Notations: The boldface front stands for a vector or a matrix. \otimes is the Kronecker product. The vectorization of \mathbf{X} is denoted by $\text{vec}(\mathbf{X})$. The Moore-Penrose inversion, transpose and conjugation of \mathbf{X} are \mathbf{X}^\dagger , \mathbf{X}^T , and \mathbf{X}^H , respectively. The l_2 norm of matrix \mathbf{X} is $\|\mathbf{X}\|_2$. The real part of complex α is $\Re(\alpha)$. $\text{diag}(\mathbf{X})$ denotes a diagonal matrix with \mathbf{X} as its diagonal elements. The expectation of x is $\mathbb{E}\{x\}$.

II. SYSTEM MODEL

We consider a wideband FDD massive MIMO system with high mobility. The UE moves at speed v . The BS antenna is a uniform planar array (UPA). The number of BS antennas is $N_t = N_v N_h$, where N_v and N_h denote the number of antennas in a row and in a column, respectively. The center frequencies of UL and DL are f^u and f^d , respectively. The DL and UL frequency band are multiplexed by orthogonal frequency division multiplex (OFDM) with N_f sub-carriers and a f_Δ subcarrier spacing.

In our work, a multi-path channel model like [10] is adopted. The number of paths is denoted by P . The complex amplitude, steering vector, Doppler frequency shift, and delay of path p are β_p , $\alpha^u(\theta_p^u, \phi_p^u)$, ω_p and τ_p , respectively. Using these channel parameters, the UL channel at a certain time t and frequency f_n^u of UE k is expressed as

$$\mathbf{h}_{k,r}^u(t, f_n^u) = \sum_{p=1}^P \beta_p^u \alpha^u(\theta_p^u, \phi_p^u) e^{-j2\pi f_n^u \tau_p^u} e^{j\omega_p^u t}, \quad (1)$$

where $f_n^u, n \in \{1, \dots, N_f\}$ is the frequency of the n -th UL subcarrier. The subscript r denotes the r -th antenna of the UE and the superscript u denotes the UL channel. In the following part of this paper, the subscripts r and k are omitted for simplicity of notations. The UL Doppler frequency shift is calculated as $\omega_p^u = v \cos \varphi_p^u f^u / c$, where $v = |\mathbf{v}|$ and φ_p^u denotes the angle between path p and \mathbf{v} . c is the speed of light. In a 3D-Cartesian coordinate system, θ_p^u, ϕ_p^u are the zenith angle and azimuth angle, respectively. Fig. 1 shows the UPA antenna configuration at the BS and the relationship between angle ϕ, φ, θ in 3D-Cartesian coordinate system.

The wideband UL channel is expressed like [6]

$$\mathbf{h}^u(t) = \sum_{p=1}^P \beta_p^u e^{-j2\pi f^u \tau_p^u} e^{j\omega_p^u t} \mathbf{r}_p^u, \quad (2)$$

where $\mathbf{r}_p^u = \mathbf{c}(\tau_p^u) \otimes \alpha^u(\theta_p^u, \phi_p^u)$ is the angle-delay structure of path p . The delay vector is denoted by $\mathbf{c}(\tau_p^u)$

$$\mathbf{c}(\tau_p^u) = e^{-j2\pi f^u f_\Delta \tau_p^u} [1 \dots e^{-j2\pi \tau_p^u (N_f - 1) f_\Delta}]^T. \quad (3)$$

Similarly, the wideband DL channel is expressed as

$$\mathbf{h}^d(t) = \sum_{p=1}^P \beta_p^d e^{-j2\pi f^d \tau_p^d} e^{j\omega_p^d t} \mathbf{r}_p^d, \quad (4)$$

where the superscript d means the DL channel. Although full channel reciprocity is not available in FDD, some frequency-independent parameters are reciprocal [12]

$$\tau_p^u = \tau_p^d, \theta_p^u = \theta_p^d, \phi_p^u = \phi_p^d, \frac{w_p^u}{w_p^d} = \frac{f^u}{f^d}. \quad (5)$$

Note that even with the same angle, the UL steering vector and DL steering vector differs. The relationship is easily obtained under UPA configuration

$$\alpha^d(\theta_p^d, \phi_p^d) = (\mathbf{R}_h(\theta_p^d, \phi_p^d) \otimes \mathbf{R}_v(\theta_p^d)) \cdot \alpha^u(\theta_p^u, \phi_p^u), \quad (6)$$

where

$$\mathbf{R}_h(\theta_p^d, \phi_p^d) = \text{diag} \left(\begin{array}{c} 1 \\ e^{j2\pi \frac{l_h(f^d - f^u)}{c} \sin \theta_p^d \sin \phi_p^d} \\ \dots \\ e^{j2\pi (N_h - 1) \frac{l_h(f^d - f^u)}{c} \sin \theta_p^d \sin \phi_p^d} \end{array} \right), \quad (7)$$

$$\mathbf{R}_v(\theta_p^d) = \text{diag} \left(\begin{array}{c} 1 \\ e^{j2\pi \frac{l_v(f^d - f^u)}{c} \cos \theta_p^d} \\ \dots \\ e^{j2\pi (N_v - 1) \frac{l_v(f^d - f^u)}{c} \cos \theta_p^d} \end{array} \right), \quad (8)$$

are the horizontal rotation matrix and vertical rotation matrix, respectively. l_v, l_h are the spacing between the antennas in vertical direction and horizontal direction, respectively. Based on (5) and (6), the DL channel parameters can be estimated from the UL channel parameters. Usually, the UL CSI is relatively easy to acquire through the sounding reference signal (SRS) [16]. Under a typical configuration in 5G new radio (NR), the SRS periodicity can be as short as 0.5 ms. The CSI delay is denoted by T_d . The following section shows the details of our framework.

III. DL CHANNEL RECONSTRUCTION FRAMEWORK

Our DL channel reconstruction framework is based on channel parameters estimated from the UL channel samples. The BS utilizes SRS to estimate the UL channel parameters. Then the BS calculates the DL channel parameters based on the partial reciprocity in FDD. A Matrix Pencil method is introduced to obtain the Doppler frequency. In order to reconstruct the DL channel, a novel wideband beamformer for pilots is proposed to facilitate the channel training and feedback process. The proposed scheme is elaborated below.

A. Uplink channel parameters estimation

The estimation of the UL channel parameters is the basis of our framework. The sparsity of the channel allows us to estimate the UL channel parameters in angle-delay domain.

The angle-delay structure \mathbf{r}_p^u can be characterized by the columns of a unitary matrix $\mathbf{Q} \in \mathbb{C}^{N_t N_f \times N_t N_f}$

$$\mathbf{Q} = \mathbf{W}(N_f)^H \otimes \mathbf{W}(N_h) \otimes \mathbf{W}(N_v), \quad (9)$$

where $\mathbf{W}(X)$ is a DFT matrix generated like [6]. The UL channel in angle-delay domain is $\hat{\mathbf{g}}^u(t) \in \mathbb{C}^{N_t N_f \times 1}$

$$\hat{\mathbf{g}}^u(t) = \mathbf{Q}^H \mathbf{h}^u(t). \quad (10)$$

Let \mathbf{q}_i be the i -th column of \mathbf{Q} and $\hat{g}_i^u(t) = \mathbf{q}_i^H \mathbf{h}^u(t)$ is the corresponding complex amplitude.

Utilizing the channel sparsity in angle-delay domain, $\mathbf{h}^u(t)$ can be approximated with the aggregation of several selected columns of \mathbf{Q} which contain most power of the channel $\mathbf{h}^u(t)$. The index set of the selected columns of \mathbf{Q} is found by

$$\mathcal{S} = \arg \min_{|\mathcal{S}|} \left\{ \sum_{l=1}^{N_L} \sum_{i \in \mathcal{S}} |\hat{g}_i^u(t_l)|^2 \geq \eta \sum_{l=1}^{N_L} |\hat{\mathbf{g}}^u(t_l)|^2 \right\}, \quad (11)$$

where η denotes the threshold. To solve the problem (11) during each prediction interval results in extra high computation resources. A fixed and median N_s is thus utilized in our algorithm to reduce the complexity. Define N_L as the number of channel samples for each parameter estimation. The size of \mathcal{S} is defined as N_s . We should note that the index set \mathcal{S} is time-varying. The argument t is omitted for simplicity in the rest of the paper. Obviously, N_s is vital to estimate the UL channel parameters. Bigger N_s leads to better estimation accuracy but higher computation complexity. Then, the UL channel can be approximated by

$$\tilde{\mathbf{h}}^u(t) = \sum_{i \in \mathcal{S}} \hat{g}_i^u(t) \mathbf{q}_i. \quad (12)$$

In fact, the complex amplitude $\hat{g}_i^u(t)$ has an implicit physical meaning. The angle-delay vector \mathbf{q}_i is utilized to characterize the angle-delay structure \mathbf{r}_p^u . The corresponding amplitude $\hat{g}_i^u(t)$ characterizes the complex gain and Doppler frequency $\beta_p^u e^{-j2\pi f^u \tau_p} e^{jw_p^u t}$. In order to estimate the Doppler frequency, $\hat{g}_i^u(t)$ is fitted with an M -order superposition of exponentials

$$\hat{g}_i^u(t) \triangleq \sum_{m=1}^M a_m^u(i) (z_m^u(i))^t, \quad (13)$$

where $(z_m^u(i))^t$ refers to the Doppler frequency $e^{jw_p^u t}$ and $a_m^u(i)$ denotes the corresponding complex amplitude. Then (12) becomes

$$\tilde{\mathbf{h}}^u(t) = \sum_{i \in \mathcal{S}} \sum_{m=1}^M a_m^u(i) (z_m^u(i))^t \mathbf{q}_i. \quad (14)$$

Due to the finite size of the DFT basis, one angle-delay vector \mathbf{q}_i may characterize multiple angle-delay structure of paths. Due to finite number of the BS antennas as well as the finite

bandwidth, M is also greater than one. The estimation of coefficients $z_m^u(i)$ is a classic polynomial parameter estimation problem which can be solved by Matrix Pencil method.

Define the prediction order as L . Then, the prediction matrices $\mathbf{P}_1(i)$, $\mathbf{P}_0(i)$ and the collection of $z_m^u(i)$ satisfy the following relationship [14]

$$\begin{cases} \mathbf{P}_0(i) = \mathbf{Z}_1(i) \mathbf{A}_u(i) \mathbf{Z}_2(i), \\ \mathbf{P}_1(i) = \mathbf{Z}_1(i) \mathbf{A}_u(i) \mathbf{Z}_0(i) \mathbf{Z}_2(i). \end{cases} \quad (15)$$

The definition of matrix $\mathbf{P}_1(i)$, $\mathbf{P}_0(i)$, \mathbf{Z}_0 , \mathbf{Z}_1 , \mathbf{Z}_2 is omitted due to lack of space and can be found in [14]. We introduce Lemma 1 of [14] below.

Lemma 1 Finding the solution to the singular generalized eigenvalue problem

$$\left(\mathbf{P}_0(i)^\dagger \mathbf{P}_1(i) \right) \mathbf{x} = z \mathbf{x}, \quad (16)$$

equals to finding $z_m^u(i)$. Each eigenvalue z equals to the corresponding $z_m^u(i)$ where \mathbf{x} is the corresponding eigenvector.

Algorithm 1 explains how to estimate the UL channel parameters which will be used for DL CSI training and channel reconstruction.

Algorithm 1 Matrix Pencil based Doppler Estimation

- 1: Initialize N_L, L, M , start time t_s , end time t_e and obtain UL channel sample in angle-delay domain $\mathbf{g}^u(t)$ as (10)
 - 2: Find a suitable N_s satisfying (11)
 - 3: **for** $t \in [t_s, t_e]$ **do**
 - 4: Obtain index set \mathcal{S}
 - 5: **for** $n_i \in [1, N_s]$ **do**
 - 6: Generate prediction matrix $\mathbf{P}_1(n_i)$, $\mathbf{P}_0(n_i)$
 - 7: Calculate the eigenvalue matrix $\mathbf{Z}_0(n_i)$ using (16)
 - 8: Update $n_i = n_i + 1$
 - 9: **end for**
 - 10: Update $t = t + 1$
 - 11: **end for**
 - 12: Return the UL angle-delay index set and Doppler frequency shift.
-

B. Extract parameters from the UL channel

Utilizing the partial reciprocity (5) and the UL channel parameters, the frequency-unrelated DL channel parameters are conveniently obtained. However, the angle-delay vectors and Doppler shifts are frequency-related. Thus the DL angle-delay vector and Doppler shifts need to be extracted from the estimated UL channel parameters. Denote the selected UL angle-delay vectors by

$$\mathbf{u}_j = \{ \mathbf{q}_i | i = i_{s_j}, j \in \{1, 2 \dots N_s\} \}, \quad (17)$$

where the index i_{s_j} is the j -th index of the UL angle-delay vector index set \mathcal{S} . Proposition 1 is introduced to extract the DL angle-delay vectors from the UL ones.

Proposition 1 The DL angle-delay vector \mathbf{d}_j is transformed from the UL angle-delay vector \mathbf{u}_j by

$$\mathbf{d}_j = (\mathbf{I}_{N_f} \otimes \mathbf{R}(\theta_j^d, \phi_j^d)) \mathbf{u}_j, j \in \{1, 2, \dots, N_s\}, \quad (18)$$

where $\mathbf{R}(\theta_j^d, \phi_j^d) = \mathbf{R}_h(\theta_j^d, \phi_j^d) \otimes \mathbf{R}_v(\theta_j^d)$.

Proof: Please refer to our full-length paper [17]. \square

Proposition 1 shows the solution to the DL angle-delay vector from the UL ones when the UE is equipped with single antenna. In practice, the UEs may have dual-polarized antennas. The generalization of our method is straightforward, as shown in Remark 1.

Remark 1 If the UEs are equipped with dual-polarized antennas, the DFT matrix $\mathbf{W}(N_t)$ becomes

$$\mathbf{W}(N_t) = \begin{bmatrix} \mathbf{W}(N_h) \otimes \mathbf{W}(N_v) & \\ & \mathbf{W}(N_h) \otimes \mathbf{W}(N_v) \end{bmatrix}.$$

Thus, the j -th DL angle-delay vector is now

$$\mathbf{d}_j = \left(\mathbf{I}_{N_f} \otimes \begin{bmatrix} \mathbf{R}(\theta_j^d, \phi_j^d) & \\ & \mathbf{R}(\theta_j^d, \phi_j^d) \end{bmatrix} \right) \mathbf{q}_i. \quad (19)$$

Moreover, the DL angle-delay vector \mathbf{d}_j has unit norm and mutual orthogonality like \mathbf{u}_j .

Lemma 2 For any $i, j = 1, \dots, N_s$, we have

$$\mathbf{d}_i^H \mathbf{d}_j = \begin{cases} 1, & i = j \\ 0, & i \neq j \end{cases}. \quad (20)$$

Proof: Please refer to our full-length paper [17]. \square

The DL Doppler frequency shifts are obtained from the UL channel parameters $z_m^u(i)$

$$e^{jw_m^d(j)} = e^{j \frac{\arccos\left(\Re\left\{\frac{z_m^u(i)}{|z_m^u(i)|}\right\}\right) f_d}{f_u}}. \quad (21)$$

C. DL pilot beamforming and CSI reconstruction

After calculating the DL Doppler frequency shifts and angle-delay vectors, the DL channel is estimated as following

$$\tilde{\mathbf{h}}^d(t) = \sum_{j=1}^{N_s} \sum_{m=1}^M a_m^d(j) e^{jw_m^d(j)t} \mathbf{d}_j, \quad (22)$$

where $a_m^d(j)$ is the m -th complex amplitude corresponding to \mathbf{d}_j , which needs to be estimated through the DL pilot training. Considering the heavy training and feedback overhead in FDD massive MIMO, we devise a beamforming matrix based on the DL channel parameters.

Based on the structure of the vectorized DL channel in (22), $\tilde{\mathbf{h}}^d(t)$ can be written as

$$\tilde{\mathbf{h}}^d(t) = \mathbf{D} \mathbf{E}(t) \mathbf{a}^d. \quad (23)$$

The matrix \mathbf{D} , \mathbf{E} and \mathbf{a}^d contain the angle-delay, Doppler and amplitude information, respectively. The DL angle-delay vector matrix $\mathbf{D} \in \mathbb{C}^{N_f N_t \times N_s}$ is generated by \mathbf{d}_j

$$\mathbf{D} = [\mathbf{d}_1 \quad \mathbf{d}_2 \quad \dots \quad \mathbf{d}_{N_s}]. \quad (24)$$

The Doppler matrix $\mathbf{E}(t) \in \mathbb{C}^{N_s \times N_s M}$ is constructed as

$$\mathbf{E}(t) = \begin{bmatrix} \mathbf{e}_1(t) & & & \\ & \mathbf{e}_2(t) & & \\ & & \ddots & \\ & & & \mathbf{e}_{N_s}(t) \end{bmatrix}, \quad (25)$$

where

$$\mathbf{e}_j(t) = [e^{jw_1^d(j)t} \quad e^{jw_2^d(j)t} \quad \dots \quad e^{jw_M^d(j)t}]. \quad (26)$$

The DL complex amplitude vector $\mathbf{a}^d \in \mathbb{C}^{N_s M \times 1}$ is

$$\mathbf{a}^d = [\mathbf{a}^d(1) \quad \mathbf{a}^d(2) \quad \dots \quad \mathbf{a}^d(N_s)]^T, \quad (27)$$

where

$$\mathbf{a}^d(j) = [a_1^d(j) \quad a_2^d(j) \quad \dots \quad a_M^d(j)]. \quad (28)$$

As the wideband vectorized channel $\tilde{\mathbf{h}}^d(t)$ can be written as (23), a beamforming matrix in spatial-frequency domain is feasible. Like [18], in our scheme, the joint spatial-frequency-Doppler beamforming is a generalized wideband concept, however, we design an extra wideband beamforming matrix. The received signal after deploying a beamforming matrix $\mathbf{F}(t)$ in spatial-frequency is

$$\tilde{\mathbf{y}}^d(t) = \tilde{\mathbf{h}}^d(t)^T \mathbf{F}(t) \mathbf{S} + \mathbf{n}(t). \quad (29)$$

The Gaussian noise vector $\mathbf{n}(t) \in \mathbb{C}^{1 \times \tau}$ has a distribution of $\mathbf{n} \sim \mathcal{CN}(0, \sigma^2 \mathbf{I})$, where σ^2 is the noise power. In the following, we elaborate how to calculate our beamforming matrix $\mathbf{F}(t)$.

First, $\mathbf{E}(t)^T \mathbf{D}^T$ has no right inverse matrix and the rank of it is N_s . Learning from (25) and (24), \mathbf{D}^T is of full row rank and $\mathbf{E}(t)^T$ is of full column rank. Therefore, there exists a right inverse matrix of \mathbf{D}^T , however, no right inverse matrix of $\mathbf{E}(t)^T$. In order to capture the Doppler effect and angle-delay information, the beamforming matrix is designed as

$$\mathbf{F}(t) = (\mathbf{D}^T)^\dagger (\mathbf{E}(t)^T)^\dagger. \quad (30)$$

Substitute $\mathbf{F}(t)$ with (30) and $\mathbf{h}^d(t)$ with (23), then (29) becomes

$$\tilde{\mathbf{y}}^d(t) = \left((\mathbf{a}^d)^T \mathbf{E}(t)^T (\mathbf{E}(t)^T)^\dagger \right) \mathbf{S} + \mathbf{n}(t). \quad (31)$$

Notice that the dimension of \mathbf{S} in (31) is $\mathbb{C}^{N_s M \times \tau}$ and no longer depends on the number of BS antennas and sub-carriers. N_s can be small due to the channel sparsity in spatial-frequency domain. M is often of small value for the complexity. Generally, the length of training sequence should be guaranteed $\tau \geq N_s M$. Without losing generality, the length of the training sequence τ satisfies $\tau = N_s M$ and \mathbf{S} is designed as a unitary matrix which can be generated from DFT sequences. Applying least-square (LS) estimation method, the unknown coefficient vector \mathbf{a}^d can be obtained by

$$\hat{\mathbf{a}}^d = \left(\mathbf{S}^T \mathbf{E}(t)^\dagger \mathbf{E}(t) \right)^\dagger \tilde{\mathbf{y}}^d(t)^T. \quad (32)$$

Then the estimated coefficient vector $\hat{\mathbf{a}}^d$ is fed back to the BS for the DL channel reconstruction (22). Furthermore, considering a T_d CSI delay, the DL channel is reconstructed at the BS as

$$\tilde{\mathbf{h}}^d(t + T_d) = \sum_{j=1}^{N_s} \sum_{m=1}^M \hat{\alpha}_m^d(j) e^{jw_m^d(j)(t+T_d)} \mathbf{d}_j. \quad (33)$$

The BS will utilize (33) for the DL precoding of the data signals.

D. The lower bound performance

In our framework, N_s determines how many angle-delay vectors are used to estimate the DL channel. It affects the complexity and prediction accuracy. The lower bound of prediction error (PE) is then derived. First, the DL channel PE is defined with the normalized mean square error (NMSE) metric as

$$\varepsilon \triangleq 10 \log \mathbb{E} \left\{ \left\| \frac{\mathbf{h}^d(t + T_d) - \tilde{\mathbf{h}}^d(t + T_d)}{\mathbf{h}^d(t + T_d)} \right\|_2^2 \right\}. \quad (34)$$

The following theorem gives the lower bound of the DL channel PE, which is derived by letting N_s take the maximum value, i.e., $N_s = N_f N_t$.

Theorem 1 *The lower bound of DL channel PE of the proposed CSI acquisition framework is*

$$\varepsilon_l = 10 \log \left(\frac{\sigma^2 N_s M}{\mathbb{E} \|\mathbf{h}^d(t + T_d)\|_2^2} \right). \quad (35)$$

Proof: Please refer to our full-length paper [17]. \square

Theorem 1 gives the lower bound of the channel PE when all the angle-delay vectors in \mathbf{Q} are taken into account. This condition may not be easy to achieve due to the huge feedback overhead and high complexity. Fortunately, the sparsity of multipath angles and delays ensures a much smaller N_s in our framework.

IV. SIMULATION RESULTS

We evaluate the proposed framework under an industrial channel model called clustered-delay-line-A (CDL-A) defined by 3GPP [10] in a rich scattering scenario. CDL-A channel model defines a multipath channel which contains a total of 23 clusters with 20 paths inside each cluster. Follow a new radio band (NR) n65 defined by [19]. The bandwidth of UL and DL are 20 MHz with a 30 kHz subcarrier spacing, implying that 51 resource blocks (RBs) are available per time slot. Under this frequency band configuration, each time slot contains 14 OFDM symbols and can be as short as 0.5 ms, which is also the SRS signal cycle length. The delay spread is 300 ns. The number of UEs is 8 and they are randomly distributed in the cell. The spacing of antennas l_v and l_h are both of half wavelength. The other parameters used in our simulation are demonstrated in Table I. We utilize Eigen Zero Forcing (EZF) [20] at the BS and apply Minimum Mean Square Error-Interference Rejection Combining (MMSE-IRC) receiver at

TABLE I
SYSTEM PARAMETERS CONFIGURATION

Physical meaning	Default value
Channel model	CDL-A
Bandwidth	20 MHz
UL carrier frequency	1.92 GHz
DL carrier frequency	2.11 GHz
Subcarrier spacing	30 kHz
Resource block	51
Number of paths	460
Transmit antenna configuration	$(N_v, N_h, P_t) = (2, 8, 2)$, polarization direction are $0^\circ, 90^\circ$
Receive antenna configuration	$(N_v, N_h, P_r) = (1, 1, 2)$, polarization direction are $\pm 45^\circ$

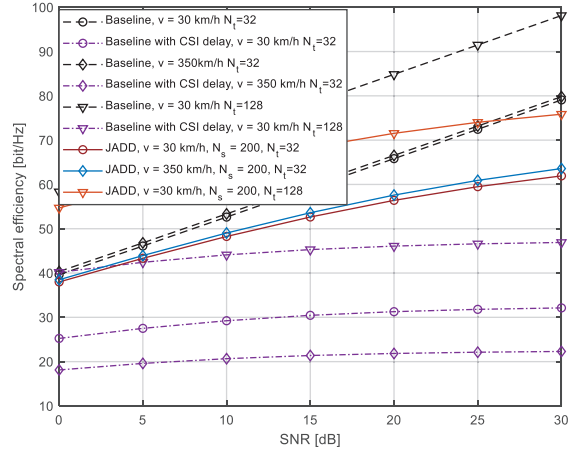


Fig. 2. SE performance vs different UE Speed and transmit antennas, noise-free channel sample, $L = 3$, $T_d = 6$ ms.

the UEs. Two performance metrics are adopted, i.e., the SE and the PE. To demonstrate the performance of our framework, we introduce two baselines following the latest codebook of 5G as benchmarks. One baseline is following [15] called the Enhanced Type II codebook where perfect CSI is known by the UEs and the BS. The other baseline is the Enhanced Type II codebook, however only delayed CSI is known by the UEs. Considering realistic application, we evaluate our framework with quantization error following the quantization method in [15]. Enhanced Type II codebook with perfect CSI refers to baseline in the rest of the paper.

Our framework is evaluated in three different scenarios in Fig. 2. Under all scenarios, the performance of the baseline with CSI delay are lower than our JADD framework. Meanwhile the performance of JADD maintains a minor performance gap compared with the baseline. Notice that there exists a small SE difference between the different mobility cases. This trivial difference is caused by the different channel sparsity under different scenarios. When the number of BS antenna $N_t = 128$, JADD also performs well. The numerical results show the superiority of our framework under different scenarios.

Fig. 3 demonstrates the PE performance under different CSI delay and different mobility scenarios. The results show that JADD performs well with high CSI delay. We may

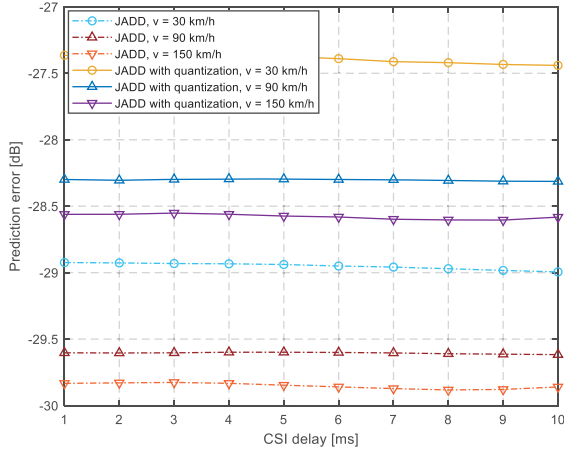


Fig. 3. PE performance vs different CSI delay, 6 bit quantization, $N_s = 200$, $L = 3$.

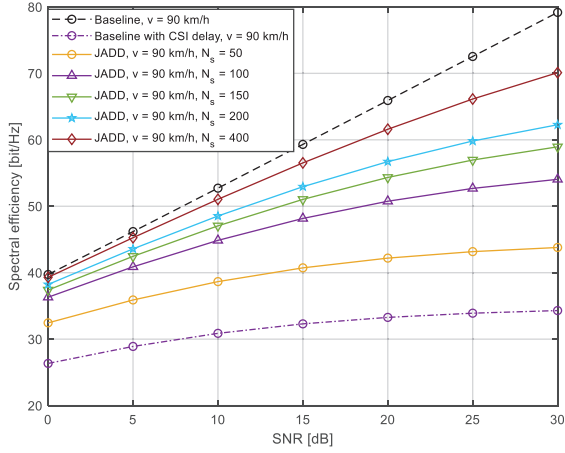


Fig. 4. SE performance vs different N_s , 6 bit quantization, $L = 3$, $T_d = 6$ ms.

conclude that our framework is robust to CSI delay even with quantization errors.

At last, we evaluate the influence of N_s on our JADD framework. Fig. 4 demonstrates the SE performance under different N_s settings. Notice that the performance of JADD always surpasses Enhanced Type II codebook no matter what the value of N_s is. The SE of JADD also quickly improves as N_s increases. However, a greater N_s brings more complexity and feedback overhead.

V. CONCLUSION

In this paper, we dealt with the CSI acquisition problem in FDD massive MIMO with high-mobility. Considering the time-varying nature and angle-delay sparsity of the multipath channel, a novel DL channel reconstruction framework JADD was proposed. Based on the partial channel reciprocity in FDD, our framework reconstruct the DL channel through the estimated UL channel parameters and predict the DL channel conveniently. Specifically, the BS and UE estimate angle-delay vectors of the UL channel and the Doppler frequency shifts by exploiting a linear estimation method called Matrix

Pencil. For the first time, we devised a wideband form of beamforming matrix in spatial-frequency-Doppler domain to reduce feedback and pilot overhead. The feedback mechanism of our framework combines the Doppler information and only includes scalar coefficients. The lower-bound of our proposed method was also derived. Simulations under a practical multipath channel model of 3GPP were carried out. The simulation results showed that our JADD framework was robust to medium to high mobility level and large CSI delays, even with quantization errors.

REFERENCES

- [1] T. L. Marzetta, "Noncooperative cellular wireless with unlimited numbers of base station antennas," *IEEE Trans. Wireless Commun.*, vol. 9, no. 11, pp. 3590–3600, 2010.
- [2] H. Q. Ngo, E. G. Larsson, and T. L. Marzetta, "Energy and spectral efficiency of very large multiuser MIMO systems," *IEEE Trans. Commun.*, vol. 61, no. 4, pp. 1436–1449, 2013.
- [3] H. Yin, D. Gesbert, M. Filippou, and Y. Liu, "A coordinated approach to channel estimation in large-scale multiple-antenna systems," *IEEE J. Sel. Areas Commun.*, vol. 31, no. 2, pp. 264–273, 2013.
- [4] B. Wang, M. Jian, F. Gao *et al.*, "Beam squint and channel estimation for wideband mmWave massive MIMO-OFDM systems," *IEEE Trans. Signal Process.*, vol. 67, no. 23, pp. 5893–5908, 2019.
- [5] Fraunhofer IIS and Fraunhofer HHI, "RP-191951: Mobility enhancements for MIMO," in *3GPP TSG RAN WG#85*, January 2019, Newport Beach California, USA.
- [6] H. Yin, H. Wang, Y. Liu, and D. Gesbert, "Addressing the curse of mobility in massive MIMO with prony-based angular-delay domain channel predictions," *IEEE J. Sel. Areas Commun.*, vol. 38, no. 12, pp. 2903–2917, 2020.
- [7] R. Wang, O. Renaudin, C. U. Bas *et al.*, "High-resolution parameter estimation for time-varying double directional V2V channel," *IEEE Trans. Veh. Technol.*, vol. 16, no. 11, pp. 7264–7275, 2017.
- [8] C. Wu, X. Yi, Y. Zhu *et al.*, "Channel prediction in high-mobility massive MIMO: From spatio-temporal autoregression to deep learning," *IEEE J. Sel. Areas Commun.*, vol. 39, no. 7, pp. 1915–1930, 2021.
- [9] Y. Han, Q. Liu, C.-K. Wen, M. Matthaiou, and X. Ma, "Tracking fdd massive mimo downlink channels by exploiting delay and angular reciprocity," *IEEE Journal of Selected Topics in Signal Processing*, vol. 13, no. 5, pp. 1062–1076, 2019.
- [10] 3GPP, *Study on channel model for frequencies from 0.5 to 100 GHz (Release 16)*. Technical Report TR 38.901, available: <http://www.3gpp.org>, 2020.
- [11] K. Hugel, K. Kalliola, J. Laurila *et al.*, "Spatial reciprocity of uplink and downlink radio channels in FDD systems," in *Proc. COST*, vol. 273, no. 2. Citeseer, 2002, p. 066.
- [12] 3GPP, *Study on elevation beamforming / Full-Dimension (FD) Multiple Input Multiple Output (MIMO) for LTE (Release 13)*. Technical Report TR 36.897, available: <http://www.3gpp.org>, 2015.
- [13] H.-W. Liang, W.-H. Chung, and S.-Y. Kuo, "FDD-RT: A simple CSI acquisition technique via channel reciprocity for FDD massive MIMO downlink," *IEEE Systems Journal*, vol. 12, no. 1, pp. 714–724, 2018.
- [14] Y. Hua and T. K. Sarkar, "Matrix pencil method for estimating parameters of exponentially damped/undamped sinusoids in noise," *IEEE Trans. Acoust., Speech, Signal Process.*, vol. 38, no. 5, pp. 814–824, 1990.
- [15] 3GPP, *NR; Physical layer procedures for data (Release 16)*. Technical Report TR 38.214, available: <http://www.3gpp.org>, 2021.
- [16] —, *NR; Physical channels and modulation (Release 16)*. Technical Report TR 38.211, available: <http://www.3gpp.org>, 2021.
- [17] Z. Qin, H. Yin, and D. Gesbert, "A partial reciprocity-based channel prediction framework for FDD massive MIMO with high mobility," *arXiv preprint arXiv:2202.05564*, 2022.
- [18] H. Yin and D. Gesbert, "A partial channel reciprocity-based codebook for wideband FDD massive MIMO," *arXiv preprint arXiv:2201.10829*, 2022.
- [19] 3GPP, *NR; Physical layer procedures for data (Release 17)*. Technical Report TR 38.104, available: <http://www.3gpp.org>, 2021.
- [20] L. Sun and M. R. McKay, "Eigen-based transceivers for the MIMO broadcast channel with semi-orthogonal user selection," *IEEE Trans. Signal Process.*, vol. 58, no. 10, pp. 5246–5261, 2010.